Published in final edited form as:
Cancer Res. 2007 October 15; 67(20): 9791–9799. doi:10.1158/0008-5472.CAN-07-0246.

Opposing Roles of Murine Duffy Antigen Receptor for Chemokine and Murine CXC Chemokine Receptor-2 Receptors in Murine Melanoma Tumor Growth

Linda W. Horton[2], **Yingchun Yu**[2], **Snjezana Zaja-Milatovic**[2], **Robert M. Strieter**[3], and **Ann Richmond**[1,2]

1 *Department of Veteran Affairs, Vanderbilt University School of Medicine, Nashville, Tennessee*

2 *Department of Cancer Biology, Vanderbilt University School of Medicine, Nashville, Tennessee*

3 *Department of Medicine, University of Virginia School of Medicine, Charlottesville, Virginia*

Abstract

The Duffy antigen receptor for chemokines (DARC) has been classified as a "silent" receptor, as it can bind CXC and CC chemokines to undergo ligand-induced receptor internalization, but is not coupled to trimeric G proteins required for the classic G protein–coupled receptor–mediated signaling. CXC chemokine receptor-2 (CXCR2) has been shown to play a major role in tumor angiogenesis. To test the hypothesis that these two chemokine receptors might play opposing roles in the growth of melanoma tumors, we developed a transgenic mouse model, where the preproendothelin promoter/enhancer (PPEP) is used to drive expression of either murine DARC (mDARC) or murine CXCR2 (mCXCR2) in endothelial cells. We show herein that the growth of melanoma tumor xenografts, established from s.c. injection of immortalized murine melanocytes overexpressing macrophage inflammatory protein-2, was inhibited or enhanced in the PPEP-mDARC and PPEP-mCXCR2 transgenic mice, respectively, compared with control mice. The early tumors formed in mDARC transgenic mice exhibited a significantly higher number of infiltrating leukocytes compared with either the control or mCXCR2 transgenic mice, suggesting a potential role for DARC expressed on endothelial cells in leukocyte migration. In addition, the tumor-associated angiogenesis in mDARC transgenic mice was reduced when compared with the control. Conversely, tumor angiogenesis was significantly increased in mCXCR2 transgenic mice. Results indicate that endothelial cell overexpression of mDARC increased leukocyte trafficking to the tumor, reduced the growth of blood vessels into the tumor, and reduced the growth rate of the tumor, whereas endothelial cell overexpression of mCXCR2 had the reverse effect on tumor angiogenesis and growth.

Introduction

Chemokines and their cognate receptors have been shown to play a major role in inflammation, wound healing, tumor growth, and metastasis. Previous research in our laboratory has focused on one of the "silent" receptors, Duffy antigen receptor for chemokines (DARC), and its role in inflammation-associated angiogenesis. Du et al. (1) showed that transgenic mice, which overexpress the Duffy antigen under the control of the preproendothelin promoter [PPEP-murine DARC (mDARC) mice], have a reduced angiogenic response to macrophage inflammatory protein-2 (MIP-2) in a corneal micropocket assay. MIP-2 is the murine functional homologue of either human CXCL8 or CXCL1. It belongs to the ELR^+ C-X-C chemokine

Requests for reprints: Ann Richmond, Department of Cancer Biology, Vanderbilt University School of Medicine, 2220 Pierce Avenue, 771 PRB, Nashville, TN 37232. Phone: 615-343-7777; Fax: 615-343-4539; E-mail: ann.richmond@vanderbilt.edu.

family in which two cysteine residues are separated by a single amino acid. C-X-C chemokines containing the amino acid sequence of glutamine-leucine-arginine (ELR) in their NH_2 terminus induce angiogenesis by binding their respective receptors and initiating a chemotactic gradient along which endothelial cells are able to migrate. These chemokines are also potent inducers of signaling cascades that lead to the activation of nuclear factor-κB and other proinflammatory molecules that further assist the angiogenic process in tissues. In addition to angiogenesis, the C-X-C chemokines are involved in the recruitment of leukocytes from the bloodstream to sites of inflammation. It seems that DARC may be involved in the maintenance of homeostasis, either by acting as a "sink" or as a "decoy," capturing the chemokine and limiting its availability to other receptors, or by binding chemokines and presenting them on the apical surface of endothelial cells to initiate the recruitment, binding, and transference of immune cells into a "stressed" environment.

Other work in our laboratories has focused on the interaction between MIP-2 and its murine receptor, murine CXCR2 (mCXCR2). We showed that blocking antibodies to CXCR2 suppress the growth of new blood vessels in rat cornea micropocket assays (2). We also showed that antibodies to CXCL1, CXCL2, and CXCL3 are capable of blocking the angiogenic response in the rat cornea as well as inhibiting the growth of melanoma tumors overexpressing each of these chemokines (1,3).

CXCR2 is expressed on leukocytes, endothelial cells, epithelial cells, and neuronal cells, whereas DARC is expressed on neuronal cells, endothelial cells, and erythrocytes. DARC is structurally very similar to CXCR2 in that both receptors contain the highly conserved cysteine residues on the extracellular loops (C51, C129, C195, and C276), which are responsible for tertiary structure configuration and formation of the chemokine binding pocket (4). However, DARC does not contain the DRYLAIVHA motif in the second intracellular loop, which is responsible for coupling the receptor to the trimeric G proteins. In contrast, DARC does, however, internalize on ligand stimulation and may play a role in endocytosis and transcytosis. Peiper et al. (5) have used DARC-transfected cell lines and showed that DARC binds chemokines and internalizes, although the DARC binding region for the chemokine melanoma growth-stimulating activity is different from the region involved in binding to CXCR2 (6). Chaudhuri et al. (7) have shown that endothelial DARC localizes to caveolae, vesicles generally associated with chemokine transcytosis.

It has been assumed that DARC does not initiate intracellular signaling, but rather serves in other capacities to maintain homeostasis. Because overexpression of mDARC in endothelial cells results in inhibition of CXCL8-mediated angiogenesis, it would stand to reason that it could also play a role during tumor development. In fact, Addison et al. (8) noted an increase in tumor necrosis and decreased vascularity in non–small cell lung cancers, which overexpress the Duffy antigen. To determine the role these two receptors play during melanoma tumor growth, we developed transgenic mice overexpressing either mDARC or mCXCR2 under the control of the preproendothelin promoter/enhancer (PPEP), which directs expression of the transgene primarily to the endothelium (PPEP-mDARC and PPEP-mCXCR2). We also used a murine melanoma model where xenografts were developed with stable polyclonal cultures of immortalized Melan-a cells, which had been transfected to overexpress the C-X-C chemokine, MIP-2. In studies described herein, melanoma tumors arising on PPEP-mDARC transgenic mice were smaller than those arising on wild-type (WT) control mice or PPEP-mCXCR2 transgenic mice. In addition, the tumors from mDARC transgenic mice contained an abundance of infiltrating lymphocytes, whereas tumors from PPEP-mCXCR2 mice had a very limited leukocyte infiltration into the tumor environment and an increased rate of tumor growth and angiogenesis. Thus, our data show that CXCR2 and DARC have opposing roles in melanoma tumor growth.

Materials and Methods

Generation of transgenic mouse lines

The generation of mDARC transgenic mice was described previously by Du et al. (1) In brief, 1.5 kb of genomic DNA encoding murine Duffy was ligated to the human growth hormone polyadenylation (hGH-polyA) sequence. This fragment was then ligated into a vector (pGEM-3Z) containing the preproendothelin promoter (PPEP-5.9 kb). The linearized DNA sequence encoding the PPEP promoter (graciously donated by Dr. Tom Quertermous, Stanford University, Stanford, CA), the murine Duffy gene, and the hGH-polyA fragment was micro-injected into fertilized ova from C57Bl/6 black female mice and transferred into pseudopregnant female B6D2 F1 foster mothers. The generation of mCXCR2 transgenic mice was done using the same procedure. A 1.6 kb *Sal*1/*Kpn*1 fragment of genomic murine CXCR2 was ligated to the hGH-polyA fragment and then ligated into the pGEM-3Z vector containing the PPEP. A linearized DNA fragment containing the promoter, the CXCR2 gene, and the hGH-polyA sequence was used for microinjection into fertilized ova before implantation into a pseudopregnant B6D2 F1 foster mother. Both microinjections were done by the Vanderbilt Cancer Center Transgenic Core. Germ-line transmission was confirmed by PCR. Mice were genotyped using methods described previously (1).

DNA extraction for genotyping of transgenic mice

Mice were weaned at 2 to 3 weeks of age and 0.5 cm of tail tissue was removed for DNA extraction. Digestion of the tissue was done using 0.5 mL proteinase K buffer [50 mmol/L Tris-HCl (pH 8.0), 100 mmol/L EDTA, 0.5% SDS], containing 25 μL proteinase K enzyme (Clontech). Tissue was digested at 60°C, overnight. After two phenol/chloroform extractions, an equal volume of 0.3 mol/L sodium acetate in 100% ethanol (pH 6.0) was added. Precipitated DNA was washed twice in 70% ethanol and a final wash in 100% ethanol. Pellets were allowed to air dry before addition of 200 μL Milli-Q water.

PCR for genotyping transgenic mice

Primers and procedures for genotyping the mDARC mice were done as outlined by Du et al. (1). The expected size of the gene fragment is 1.0 kb. The same forward primer (PPEP1) was used for both the DARC and CXCR2 transgenic lines, as both contain the same preproendothelin promoter region (5′-CCTGGATTGTCAGACGGC-3′). A second primer, named A1487, was designed at the junction of the CXCR2 and the hGH-polyA fragment (5′-TAGAGGGTAGTAGAGGTGTT-3′). PCR conditions were as follows: 95°C for 1 min (initial denaturation), 95°C for 30 s (denaturation); 69°C for 1 min 30 s (elongation and annealing); repeat steps 2 and 3 for 29 cycles; 69°C for 10 min (final extension). PCR products were analyzed by agarose gel electrophoresis with ethidium bromide staining. The fragment obtained was 2.1 kb.

Creation and culture of Mela-MIP-2$^+$ murine melanoma cells

A 446-bp fragment of MIP-2 was inserted into the *Eco*RI and *Sma*I restriction sites of the pIRES2-EGFP vector containing the G418 resistance gene. The construct was linearized with *BSa*I and transfected into Melan-a murine melanoma cells using Fugene 6 (Roche), according to the manufacturer's instructions. Green fluorescent protein–positive cells were then sorted by fluorescence-activated cell sorting (FACS). Stable transfectants were grown in RPMI 1640 supplemented with 10% FBS (heat inactivated at 56°C for 30 min), 800 μg/mL G418, 2 mmol/L L-glutamine, 100 IU/mL penicillin, and 1 mg/mL streptomycin. Cells were maintained in a 37°C incubator with 10% CO_2/90% air. Cells were harvested with enzyme-free dissociation buffer (Life Technologies), washed, counted by trypan blue exclusion, and resuspended to a final concentration of 10×10^6/200 μL of sterile saline.

Generation of Mela-MIP-2$^+$ tumors

A minimum of five mice of each genotype (mDARC, mCXCR2, and WT) were injected s.c. in the right rear flank with 10×10^6 cells in 200 μL of sterile saline. Tumor measurements were made with calipers every 2 days after the tumors became palpable (10–15 days). When the first tumor reached the maximum allowable size in any dimension (1.5 cm), all mice were sacrificed by CO_2 inhalation, tumors were excised, and volume was determined by fluid displacement. The tumors were fixed in 4% paraformaldehyde for 24 h before being embedded in paraffin, cut, and mounted onto slides. The experiment was repeated once. All aspects of the animal experiments were approved by the Vanderbilt Institutional Animal Care and Use Committee under assigned protocol number V05/331.

Immunohistochemistry

Slides were stained either in the Vanderbilt Immunohistochemistry Core or in our own laboratory using protocols previously established. Rabbit antibody to mCXCR2 (2) was used at a dilution of 1:50, followed by the Vectastain ABC Development System (Vector Laboratories). mDARC was detected using a sheep anti-murine Duffy antibody at a 1:50 dilution as described previously by Du et al. (1). Proliferating cell nuclear antigen (PCNA) and S-100 antibodies were purchased from DAKO and used at a 1:400 dilution followed by the DAKO Envision+ Substrate System (DAKO) to examine actively replicating cells and tumor cells, respectively. The Periodic Acid Schiff stain (PAS) was done by the Vanderbilt Ingram Cancer Center Immunohistochemistry Core and used to detect PAS-positive vessels. CD31 [platelet/endothelial cell adhesion molecule-1 (PECAM-1)] antibody from Santa Cruz Biotechnology was used at a 1:400 dilution followed by the Vectastain ABC Elite System to visualize blood vessels. Macrophages were detected with F4/80 antibody (Serotec, Inc.) at a 1:100 dilution followed by the Vectastain ABC Elite Substrate System. A pan-lymphocyte stain was performed using both antibodies to CD3 (DAKO) and CD45R (BD Biosciences) on the same tissue section. The Vectastain ABC Elite Substrate System was used to visualize cells of the lymphocytic lineage. Finally, Ly6G antibody (Santa Cruz Biotechnology) was used to detect neutrophils, followed again by the Vectastain ABC Elite Substrate System. All slides for all stains were treated in a heated Target Retrieval Solution (DAKO) before staining with the primary antibodies. Terminal deoxynucleotidyl transferase–mediated dUTP nick end labeling (TUNEL) assay was done using the DeadEnd Fluorometric TUNEL System from Promega according to the manufacturer's instructions and viewed on a Nikon Labophot fluorescent microscope at ×40 magnification.

Quantification of cell numbers in tissue samples

All images were taken using a Nikon Labophot scope with attached Nikon Spot camera and the Spot Advanced software. Unless otherwise noted, all photos were taken at ×40 magnification. Each tumor was sectioned at two different depths and stained as described above, and a minimum of 10 fields at each depth were photographed. ImagePro Plus 5.1 software was used to detect and quantify specific areas of immunostaining. Mean area, density, and percentage of stain were calculated using Microsoft Excel and presented in graph form that includes SE and statistical significance as determined by the Student's *t* test.

Flow cytometry

Tumors were excised, minced, and pressed through a 70-mm nylon cell strainer (Falcon #352350, VWR) using the rubber end of a 3 cc syringe plunger and 2 mL of digestion buffer (0.1 mg/mL hyaluronidase, 0.2 mg/mL DNase type IV, 10 mg/mL collagenase type IV, in RPMI). The resulting single-cell suspension was collected by centrifugation and washed twice to remove enzymes and lipid contaminants. RBC were lysed using ACK lysing buffer [0.15 mol/L NH_4Cl, 1 mol/L $KHCO_3$, 0.1 mmol/L Na_2EDTA (pH 7.2)] for 2 min on ice. Cells were

placed into a 150-mm tissue culture dish (Corning #08-772-24, Fisher Scientific) and incubated at 37°C and 5% CO_2 for 1 h. Nonadherent cells were removed, counted, and resuspended in PBS with 1% fetal bovine serum (FBS) at a concentration of 1×10^6/mL. One milliliter of the cell suspension was placed into each cytometry tube, on ice. Primary antibodies conjugated to FITC were added at dilutions recommended by the manufacturer. Cells were incubated on ice, in the dark, for 1 h before washing. The cell pellets were resuspended in 1 mL ice-cold PBS containing 2% FBS and analyzed using a FacStar fluorescent reader. Antibodies used were hamster anti-mouse CD3e (FITC control), rat anti-mouse CD22 (eBioscience), rat anti-mouse CD8a, rat anti-mouse CD4 (BD Biosciences). MOPC-21 (Abcam) was used as an isotypic control and F4/80 antibody to a macrophage surface marker (Serotec) was used to confirm the elimination of the majority of adherent cells.

Statistical analysis of data

Differences in groups were evaluated using the paired two-sided Student's *t* test.

Results

To determine the effects of expression of mCXCR2 or mDARC on endothelial cells during melanoma tumor growth, Mela-MIP-2^+ cells were injected s.c. into 5 PPEP-mCXCR2 transgenic mice, 5 PPEP-mDARC transgenic mice, and 6 WT littermates. The age of the mice varied from 4 to 6 months and a similar number of males and females were used in each group of mice. Tumor measurements were made twice weekly and all tumors were excised when the first tumor reached the maximum allowable size of 1.5 cm in any dimension. This maximal tumor size occurred first in the CXCR2 transgenic mice, at 42 and 45 days, respectively, after implantation for the two experiments. At that time point, all tumors were removed and weighed and the mean tumor volume was determined by fluid displacement (Fig. 1*A*). Tumors from the mDARC transgenic mice were significantly smaller (55% smaller) than those from the WT controls ($P < 0.05$). In contrast, tumors removed from the mCXCR2 transgenic mice showed a highly significant increase in tumor size (over 61% increase) than seen in the WT animals ($P < 0.005$).

Because expression of both transgenes is under the control of the preproendothelin promoter (PPEP), enhanced expression of mCXCR2 and mDARC transgenes was expected to be primarily on endothelial cells. To confirm endothelial cell overexpression of the transgene, excised tumors were embedded in paraffin, sectioned, and stained with polyclonal antibodies to either mDARC or mCXCR2. Compared with WT mice (Fig. 1*C* and *E*), CXCR2 was highly expressed in the endothelium of tumors from the PPEP-mCXCR2 transgenic mice (Fig. 2*B*) and mDARC was highly expressed in tumor endothelial cells from PPEP-mDARC transgenic mice (Fig. 2*D*). The genotype of each tumor-bearing mouse was confirmed by repeat PCR at the time of tumor removal (Fig. 2*F* and *G*).

As mCXCR2 is the receptor for a variety of C-X-C ELR$^+$ angiogenic chemokines, including MIP-2, we postulated that any increase in tumor size in the mCXCR2 transgenic mice was at least partially due to the enhanced angiogenesis required to support tumor growth. Tumor sections were stained with antibody to PECAM-1 and vessel density was quantitated using ImagePro Plus software, as described in Materials and Methods. We observed a significant increase (19%) in the number of PECAM-1–positive vessels in tumors from mCXCR2 transgenic mice (Fig. 2*C*) compared with tumors from WT control mice (Fig. 2*A*), whereas PECAM-1–positive vessels were significantly reduced (41%) in the tumors from mDARC transgenic mice (Fig. 2*B*) compared with tumors obtained from WT mice. PECAM-1–positive vessels in tumors from mCXCR2 transgenic mice were >2-fold more numerous than for tumors on mDARC transgenic mice (Fig. 2*E*). Thus, the overexpression of the mDARC transgene greatly reduced the angiogenic response to the MIP-2–producing tumor. Using a TUNEL assay,

we further confirmed that there was not an increased number of apoptotic cells in the DARC tumor over that seen in the CXCR2 transgenic mouse tumor so growth inhibition was not due to a higher rate of cell death (data not shown).

Vascular channels have been described by Maniotis et al. (9) in aggressive primary melanoma tumors. To determine if these PAS-positive vessels were present in the melanoma tumors, we stained sections of melanoma tumor xenografts arising in mDARC, mCXCR2, and WT transgenic mice with PAS. We observed these vessels almost exclusively in the mCXCR2 tumors, indicating that the overexpression of the mCXCR2 transgene could potentially enhance the growth and development of this supplemental network of vessels (Fig. 2*D*). In many instances, these microvessels actually seemed to surround individual tumor cells or clusters of tumor cells, leading further support to the hypothesis that these vessels may function as an alternative source of nutrition to the growing tumor. Very few PAS-positive vessels were found in tumors arising in WT or mDARC transgenic mice. Future research in our laboratories and others may lead to a better understanding of the role of these vessels in the tumor environment.

Based on PCNA staining of the tissue sections, an unexpected finding was that there was no significant difference in the number of proliferating cells between the larger mCXCR2 transgene-expressing tumors and the smaller mDARC transgene-expressing at the time tumors were removed. PCNA staining for tumors on both mDARC and mCXCR2 transgenic mice was significantly higher than the WT tumor controls (55% and 84%, respectively; Fig. 3). For tumor xenografts arising on mCXCR2 transgenic mice, S-100 staining confirmed that the PCNA-positive cells were also S-100 positive. S-100 staining of the tumor sections from mDARC transgenic mice showed a reduced number of tumor cells that were S-100 positive per unit area, suggesting that other cell populations present within the DARC transgenic mice were expanding.

Sections of tumor from WT, mDARC, and mCXCR2 transgenic mice were stained with a pan-lymphocyte antibody cocktail (CD3/CD45; Fig. 4*D*). The total lymphocyte density in the tumor from mDARC transgenic mice (Fig. 4*B*) was dramatically higher than that seen in either the tumors from WT mice (Fig. 4*A*) or mCXCR2 transgenic mice (Fig. 4*C*).

To determine if a specific subset of lymphocytes was dominating the tumor infiltrate, we used flow cytometry to stain single-cell suspensions of mDARC-overexpressing tumors. We used cells from the WT tumor as a control population. Results of the fluorescence analysis of tumors from mDARC transgenic mice using anti-CD4, anti-CD8, and anti-CD22 antibodies suggested that lymphocytes might be included in the proliferative population because $CD8^+$ cytotoxic lymphocytes and $CD4^+$ T_h lymphocytes were significantly higher in tumors from mDARC-overexpressing mice than in tumors arising in the WT mice. The B-cell populations were almost identical in tumors arising on both genotypes (Fig. 4*E*).

There were also a significantly higher number of macrophages in tumors arising on mDARC transgenic mice (3.6-fold; $P < 0.0005$; Fig. 5*B*) over that seen in either the WT control mice (Fig. 5*A* and *D*) or the mCXCR2 transgenic mice (Fig. 5*C*). The presence of large numbers of infiltrating lymphocytes in mDARC transgenic mice adds weight to the possibility that these macrophages within the mDARC transgenic tumors are serving as antigen-presenting cells and that lymphocytes are the proliferating population.

Tumors from all three groups of animals contained only a few infiltrating neutrophils with no significant difference between mouse genotypes noted (data not shown).

Discussion

In the past 50 years, many functions have been proposed and/or shown for DARC. It was originally identified in 1950 by Cutbush et al. (10) and described as an alloantibody against an antigen in a hemophiliac patient (Mr. Duffy), who had received multiple blood transfusions. One year later, it was described by Iken et al. (11) as a set of small blood group antigens called fy^a and fy^b. In 1975, Miller et al. determined that these same blood group antigens served as the receptors for the malarial parasite, *Plasmodium vivax*, because antibodies to the blood group alleles prohibited binding and entry of the parasite into RBCs. In populations of individuals with the $fy^{(a-/b-)}$ phenotype, the incidence of malarial invasions was extremely rare, leading support to the premise that these alleles served as the point of entry for this parasite (12–14).

In 1991, Darbonne et al. made the observation that a novel new chemokine receptor on RBCs seemed to bind a wide variety of C-X-C and C-C chemokines including interleukin-8 (IL-8; CXCL8), melanoma growth stimulatory activity (CXCL1), as well as RANTES (CCL5) and monocyte chemotactic protein-1 (CCL2), with equal specificity (15–17). When anti-Fy^a antibody was used to pretreat RBCs before the addition of CXCL8 chemokine, the chemokine binding to RBCs was eliminated. This pointed to the conclusion that both chemokines and the *P. vivax* parasite used the same receptor (16,18–20). Darbonne et al. (17) proposed that DARC on RBCs could possibly function to inactivate circulating chemokines by acting as a “sink,” removing excess chemokines from the bloodstream. Subsequent research localized DARC to endothelial cells on post-capillary venules of various tissues, where DARC binds inflammatory chemokines (17–21).

Structural analysis of the DARC receptor has shown it to be very similar to the “classic” G protein–coupled receptors. DARC is a seven-transmembrane protein, which shares the conserved cysteine and proline residues responsible for formation of the chemokine binding pocket and the transmembrane structure, respectively. However, DARC lacks the DRY motif in the second intracellular loop, preventing it from binding to trimeric G proteins. In addition, on ligand binding, no phenotypic change is noted in the endothelial cells that would otherwise indicate activation of signaling pathways (4,21,22). Cells transfected with DARC do, however, internalize radiolabeled ligand, indicating that ligand binding does initiate receptor internalization (5). DARC contains five conserved phosphorylation sites in the COOH-terminal domain. This is far fewer than seen in the classic chemokine receptors, but it cannot be ruled out that signaling occurs through these phosphorylation sites (23).

Another proposed function of DARC is the movement of chemotactic chemokines from the basolateral surface of endothelial cells to the luminal surface, where they make the chemokines available to circulating leukocytes bearing chemokine receptors (24–26). It is currently unknown whether DARC itself presents the chemokine or if it passes the chemokine to adjacent glycosaminoglycans, which are abundant on the luminal surface of endothelial cells (27).

Bandyopadhyay et al. recently determined that DARC interacts with another tetraspanin cell surface protein known as the leukocyte cell surface marker CD82, or KAI1, on prostate tumor cells leading to suppression of metastasis (28–30). DARC has been found to be up-regulated on endothelial cells in the kidneys of children with renal disease and during acute renal rejection (31,32). Lee et al. (25) has shown that DARC seems to facilitate the movement of chemokine across the endothelium for presentation on the luminal surface of the cells in a lung inflammation model. Thus, DARC seems to be involved in numerous activities relative to tumor growth and inflammation.

Enhanced expression of DARC in breast cancer cells has been shown by Wang et al. (33) to inhibit the growth and the metastatic potential of these cells. Alternatively, depletion or blockage of the CXCR2 receptor inhibited growth of pancreatic, lung, and prostate cancers, as

well as giant cell arteritis (34–37). Previous research in our laboratory determined that DARC could function as a chemokine "decoy" and prevent binding of the chemotactic chemokine, MIP-2, to its cognate receptor, CXCR2 (1). Although there was marked inhibition of angiogenesis in an inflammatory response, it was unknown if this same response would occur during melanoma tumorigenesis.

Chemokines are a major regulator of both angiogenesis (38) and leukocyte trafficking (39), so our use of transgenic mice, which overexpressed either the mCXCR2 or the mDARC receptors, allowed us to investigate tumor growth and tumor-associated angiogenesis when either of these receptors was overexpressed. We also used murine melanoma cells, which had been stably transfected with the C-X-C, ELR^+ chemokine, MIP-2. Based on our prior work, it was expected that angiogenesis would be enhanced when the receptor for the chemotactic MIP-2 chemokine (CXCR2) was overexpressed. Varney et al. (40,41) noted that malignant melanoma cells had constitutively active CXCR2 whose incidence increased as the metastatic potential increased. Li et al. (42) found increased levels of CXCR2 with increased metastatic potential in colon carcinoma. Reiland et al. (43) determined that increased CXCR2 in prostate carcinoma cells enhanced invasion and chemotaxis and Metzner et al. (44) found increased expression of CXCR2 in epidermoid carcinoma cells over that seen in normal keratinocytes. Finally, Murphy et al. has shown that increased expression of CXCR2 correlates with increased cell proliferation and microvessel density in prostate carcinoma. Based on these findings, it would seem that increased levels of CXCR2 expression in malignant cells would lead to a higher metastatic potential and increased rate of growth due to enhanced angiogenesis.

Overexpression of the DARC receptor was expected to decrease angiogenesis by competing with autologous CXCR2 receptors for the angiogenic MIP-2 chemokine ligand. Indeed, we observed that tumors arising on mice that overexpressed the mCXCR2 receptor on endothelial cells had a marked increase in the number of blood vessels, whereas the tumors arising on mDARC transgenic mice had a marked decrease in tumor vasculature when compared with tumors originating in the WT mice, supporting the hypothesis that these receptors have opposing roles in angiogenesis. Furthermore, based on work described here, it would seem that overexpression of mDARC not only inhibited angiogenesis but also tumor growth.

Tumor sections stained with PAS to determine the presence or absence of an alternative vessel system described previously by Maniotis et al. (9) indicated that this network of vessels was much more predominant in the mCXCR2 transgenic mouse tumors. Although the function of this microvessel system is still unknown, it is feasible to propose that they may provide an alternate source of nutrition and thereby further enhance the growth of the mCXCR2 tumors.

Our data also show that DARC may play a role in immune cell recruitment to the tumor that could potentially contribute to the inhibition of tumor growth. The dramatic increase in the number of intratumoral T lymphocytes and macrophages over that seen in either the mCXCR2-overexpressing mice or their WT littermates indicates that inhibition of tumor growth may be due in part to the recruitment of immunocompetent cells in addition to the inhibition of angiogenesis. Using a transendothelial cell migration assay, Lee et al. (25) showed that a monolayer of human umbilical vascular endothelial cells that expressed the Duffy antigen permitted a significant increase in the number of migrating leukocytes in response to IL-8 compared with cells that did not express the Duffy antigen. Their data would seem to support the premise that Duffy antigen is an important component of chemokine-mediated leukocyte migration.

Because tumors that arise in the mCXCR2 and the mDARC mice showed similar levels of proliferating cells, both higher than that seen in the WT mouse tumor, we investigated various cells within each tumor to determine which populations were proliferating. Staining with S-100

indicated that the vast majority of tumor cells in the mCXCR2-overexpressing tumors were proliferating (data not shown). Although there were also a large number of proliferating melanoma cells in the mDARC-overexpressing tumor, the abundance of cells of T-cell lineage suggests that T cells contribute to the proliferating population in these transgenic mice. In further support of our hypothesis, only the mDARC-overexpressing tumors contained enhanced numbers of infiltrating macrophages. As both CD4 and CD8 subsets of T lymphocytes require antigen presentation in conjunction with the class II MHC molecule, perhaps these observed macrophages are functioning in the role of antigen presentation. There was no difference in the number of B cells in the mDARC and the WT tumors, as observed by fluorescent analysis. It is rather intriguing to note the significant decrease in the number of infiltrating lymphocytes in the mCXCR2 transgenic mouse tumor. These mice express levels of endogenous mDARC comparable with WT control mouse tumors, so the decreased leukocyte infiltration in PPEP-mCXCR2 transgenic mice is likely due to the higher level of CXCR2 expression in endothelial cells, which competes with mDARC for C-X-C chemokines, making them less available to mDARC for presentation to leukocytes to facilitate leukocyte trafficking.

Although it is still unclear whether DARC plays an active role in chemokine function or only serves as a “decoy” receptor or chemokine “sink,” it is obvious from our research that an overabundance of the mDARC receptor limits the early growth rate of the tumor in the mouse model. It must also be noted that although no intracellular signaling has been attributed to DARC, there is definitely a directed movement of the chemokine-bound DARC receptor from the basolateral surface to the luminal surface of the endothelial cell, indicating a functional role for this receptor. In addition, some signals may be enlisted to recruit DARC to the caveolae, as DARC travels from the basal surface to the luminal surface (7,25).

Although we are unable to explain their presence or function, it is also noteworthy that we observed a large number of PAS-positive vessels in the tumors from CXCR2-overexpressing mice over that seen in either the tumors from mDARC transgenic mice or the WT littermates. Using PAS staining, Maniotis et al. identified and described the formation of patterned vascular channels found in the most aggressive primary intraocular (uveal) melanomas and their metastases and in metastatic cutaneous melanomas (9,45). Their data revealed that these patterned vascular channels in aggressive primary and metastatic melanoma are different from endothelial-derived angiogenic vessels and the tumor cells that generate these channels have aberrant gene expression associated with embryonic stem cells. These vessels may contribute to enhanced growth of melanoma tissue on the PPEP-mCXCR2 transgenic mice.

Data presented here indicate that overexpression of CXCR2 enhances tumor growth in part by enhancing tumor angiogenesis. We also show that the Duffy antigen plays a dual role in the melanoma tumor environment: (*a*) inhibition of angiogenesis by competing with CXCR2 for the angiogenic ligands and (*b*) the possible recruitment of immunocompetent cells into the tumor environment. Based on our data, one might expect that Duffy-negative individuals might have a higher incidence of cancer or be subject to more rapid tumor growth when tumors arise. Indeed, a study by Shen et al. in 2006 compared the incidence of prostate tumor growth in $DARC^{-/-}$ mice and $DARC^{+/+}$ mice. Although the absence of the DARC receptor did not seem to play a role in the initiation of prostate tumors, it had a profound affect on the subsequent growth rate of the tumor. $DARC^{-/-}$ mice had increased levels of angiogenesis, an increased level of ELR^{+} angiogenic chemokines, and a faster rate of growth. Shen et al. concluded that DARC may function to clear angiogenic chemokines from the tumor, leading to a decreased rate of tumor growth. Seventy percent of African American men carry the $fy^{(a-b-)}$ phenotype and African American men have a higher incidence of prostate cancer than Caucasian men, suggesting that loss of Duffy on RBC is associated with the higher incidence of prostate cancer in males of African descent (46).

Our studies suggest that DARC may possibly capture chemotactic chemokines at the basolateral surface of the endothelial cells, internalize them, and transport them to the apical, or luminal, surface of the endothelial cells. In this manner, leukocytes flowing in the bloodstream adhere to the endothelial cell in an integrin-dependent process and extravasate through the endothelium to underlying tissues where they migrate along a chemokine gradient to the target site. Aternatively, DARC expressed on the luminal surface of the endothelium may find chemokines circulating in the bloodstream and present the chemokine in concert with glycosaminoglycans to leukocytes. These leukocytes could then migrate through the endothelium and chemotax toward the chemokine gradient generated by the tumor.

Our data would support these findings and offer further explanation for enhanced tumor growth in DARC$^{-/-}$ mice through the infiltration of immunocompetent cells. Both enhanced angiogenesis and decreased immune response would most probably lead to a poor prognosis in individuals lacking the DARC.

Acknowledgements

Grant support: Department of Veterans Affairs Merit grant AS 522, NIH grant CA34589, and the Vanderbilt Ingram Cancer Center.

We thank Kevin Vo and Sarah Palmer for the invaluable assistance with all animal work associated with this study.

References

1. Du J, Luan J, Liu H, et al. Potential role for Duffy antigen chemokine-binding protein in angiogenesis and maintenance of homeostasis in response to stress. J Leukoc Biol 2002;71:141–53. [PubMed: 11781390]
2. Addison CL, Daniel TO, Burdick MD, et al. The CXC chemokine receptor 2, CXCR2, is the putative receptor for ELR^{+} CXC chemokine-induced angiogenic activity. J Immunol 2000;165:5269–77. [PubMed: 11046061]
3. Owen JD, Strieter R, Burdick M, et al. Enhanced tumor-forming capacity for immortalized melanocytes expressing melanoma growth stimulatory activity/growth-regulated cytokine β and γ proteins. Int J Cancer 1997;73:94–103. [PubMed: 9334815]
4. de Brevern AG, Wong H, Tournamille C, Colin Y, Le Van Kim C, Etchebest C. A structural model of a seven-transmembrane helix receptor: the Duffy antigen/receptor for chemokine (DARC). Biochim Biophys Acta 2005;1724:288–306. [PubMed: 16046070]
5. Peiper SC, Wang ZX, Neote K, et al. The Duffy antigen/receptor for chemokines (DARC) is expressed in endothelial cells of Duffy negative individuals who lack the erythrocyte receptor. J Exp Med 1995;181:1311–7. [PubMed: 7699323]
6. Hesselgesser J, Chitnis CE, Miller LH, et al. A mutant of melanoma growth stimulating activity does not activate neutrophils but blocks erythrocyte invasion by malaria. J Biol Chem 1995;270:11472–6. [PubMed: 7744785]
7. Chaudhuri A, Nielsen S, Elkjaer ML, Zbrzezna V, Fang F, Pogo AO. Detection of Duffy antigen in the plasma membranes and caveolae of vascular endothelial and epithelial cells of nonerythroid organs. Blood 1997;89:701–12. [PubMed: 9002974]
8. Addison CL, Belperio JA, Burdick MD, Strieter RM. Overexpression of the duffy antigen receptor for chemokines (DARC) by NSCLC tumor cells results in increased tumor necrosis. BMC Cancer 2004;4:28. [PubMed: 15214968]
9. Maniotis AJ, Folberg R, Hess A, et al. Vascular channel formation by human melanoma cells *in vivo* and *in vitro*: vasculogenic mimicry. Am J Pathol 1999;155:739–52. [PubMed: 10487832]
10. Cutbush M, Mollison PL. The Duffy blood group system. Heredity 1950;4:383–9. [PubMed: 14802995]
11. Ikin EW, Mourant AE, Pettenkofer HJ, Blumenthal G. Discovery of the expected haemagglutinin, anti-Fyb. Nature 1951;168:1077–8. [PubMed: 14910641]

12. Miller LH, Mason SJ, Dvorak JA, McGinniss MH, Rothman IK. Erythrocyte receptors for (Plasmodium knowlesi) malaria: Duffy blood group determinants. Science 1975;189:561–3. [PubMed: 1145213]
13. Mason SJ, Miller LH, Shiroishi T, Dvorak JA, McGinniss MH. The Duffy blood group determinants: their role in the susceptibility of human and animal erythrocytes to Plasmodium knowlesi malaria. Br J Haematol 1977;36:327–35. [PubMed: 70210]
14. Aikawa M, Miller LH, Johnson J, Rabbege J. Erythrocyte entry by malarial parasites. A moving junction between erythrocyte and parasite. J Cell Biol 1978;77:72–82. [PubMed: 96121]
15. Horuk R, Colby TJ, Darbonne WC, Schall TJ, Neote K. The human erythrocyte inflammatory peptide (chemokine) receptor. Biochemical characterization, solubilization, and development of a binding assay for the soluble receptor. Biochemistry 1993;32:5733–8. [PubMed: 8389192]
16. Neote K, Darbonne W, Ogez J, Horuk R, Schall TJ. Identification of a promiscuous inflammatory peptide receptor on the surface of red blood cells. J Biol Chem 1993;268:12247–9. [PubMed: 8389755]
17. Darbonne WC, Rice GC, Mohler MA, et al. Red blood cells are a sink for interleukin 8, a leukocyte chemotaxin. J Clin Invest 1991;88:1362–9. [PubMed: 1918386]
18. Hadley TJ, Peiper SC. From malaria to chemokine receptor: the emerging physiologic role of the Duffy blood group antigen. Blood 1997;89:3077–91. [PubMed: 9129009]
19. Chaudhuri A, Zbrzezna V, Polyakova J, Pogo AO, Hesselgesser J, Horuk R. Expression of the Duffy antigen in K562 cells. Evidence that it is the human erythrocyte chemokine receptor. J Biol Chem 1994;269:7835–8. [PubMed: 8132497]
20. Neote K, Mak JY, Kolakowski LF Jr, Schall TJ. Functional and biochemical analysis of the cloned Duffy antigen: identity with the red blood cell chemokine receptor. Blood 1994;84:44–52. [PubMed: 7517217]
21. Tournamille C, Blancher A, Le Van Kim C, et al. Sequence, evolution, and ligand binding properties of mammalian Duffy antigen/receptor for chemokines. Immunogenetics 2004;55:682–94. [PubMed: 14712331]
22. Tournamille C, Filipe A, Wasniowska K, et al. Structure-function analysis of the extracellular domains of the Duffy antigen/receptor for chemokines: characterization of antibody and chemokine binding sites. Br J Haematol 2003;122:1014–23. [PubMed: 12956774]
23. Horuk R. Molecular properties of the chemokine receptor family. Trends Pharmacol Sci 1994;15:159–65. [PubMed: 7754534]
24. Mantovani A, Bonecchi R, Locati M. Tuning inflammation and immunity by chemokine sequestration: decoys and more. Nat Rev Immunol 2006;6:907–18. [PubMed: 17124512]
25. Lee JS, Frevert CW, Wurfel MM, et al. Duffy antigen facilitates movement of chemokine across the endothelium *in vitro* and promotes neutrophil transmigration *in vitro* and *in vivo*. J Immunol 2003;170:5244–51. [PubMed: 12734373]
26. Haraldsen G, Rot A. Coy decoy with a new ploy: interceptor controls the levels of homeostatic chemokines. Eur J Immunol 2006;36:1659–61. [PubMed: 16791884]
27. Rosenberg RD, Shworak NW, Liu J, Schwartz JJ, Zhang L. Heparan sulfate proteoglycans of the cardiovascular system. Specific structures emerge but how is synthesis regulated? J Clin Invest 1997;100:S67–75. [PubMed: 9413405]
28. Bandyopadhyay S, Zhan R, Chaudhuri A, et al. Interaction of KAI1 on tumor cells with DARC on vascular endothelium leads to metastasis suppression. Nat Med 2006;12:933–8. [PubMed: 16862154]
29. Rinker-Schaeffer CW, Hickson JA. Stopping cancer before it colonizes. Nat Med 2006;12:887–8. [PubMed: 16892031]
30. Zijlstra A, Quigley JP. The DARC side of metastasis: shining a light on KAI1-mediated metastasis suppression in the vascular tunnel. Cancer Cell 2006;10:177–8. [PubMed: 16959609]
31. Liu XH, Hadley TJ, Xu L, Peiper SC, Ray PE. Up-regulation of Duffy antigen receptor expression in children with renal disease. Kidney Int 1999;55:1491–500. [PubMed: 10201015]
32. Segerer S, Regele H, Mac KM, et al. The Duffy antigen receptor for chemokines is up-regulated during acute renal transplant rejection and crescentic glomerulonephritis. Kidney Int 2000;58:1546–56. [PubMed: 11012889]

33. Wang J, Ou ZL, Hou YF, et al. Enhanced expression of Duffy antigen receptor for chemokines by breast cancer cells attenuates growth and metastasis potential. Oncogene 2006;25:7201–11. [PubMed: 16785997]
34. Bruhl H, Vielhauer V, Weiss M, Mack M, Schlondorff D, Segerer S. Expression of DARC, CXCR3, and CCR5 in giant cell arteritis. Rheumatology (Oxford) 2005;44:309–13. [PubMed: 15572394]
35. Wente MN, Keane MP, Burdick MD, et al. Blockade of the chemokine receptor CXCR2 inhibits pancreatic cancer cell-induced angiogenesis. Cancer Lett 2006;241:221–7. [PubMed: 16458421]
36. Keane MP, Belperio JA, Xue YY, Burdick MD, Strieter RM. Depletion of CXCR2 inhibits tumor growth and angiogenesis in a murine model of lung cancer. J Immunol 2004;172:2853–60. [PubMed: 14978086]
37. Murphy C, McGurk M, Pettigrew J, et al. Nonapical and cytoplasmic expression of interleukin-8, CXCR1, and CXCR2 correlates with cell proliferation and microvessel density in prostate cancer. Clin Cancer Res 2005;11:4117–27. [PubMed: 15930347]
38. Rosenkilde MM, Schwartz TW. The chemokine system—a major regulator of angiogenesis in health and disease. APMIS 2004;112:481–95. [PubMed: 15563311]
39. Middleton J, Patterson AM, Gardner L, Schmutz C, Ashton BA. Leukocyte extravasation: chemokine transport and presentation by the endothelium. Blood 2002;100:3853–60. [PubMed: 12433694]
40. Varney ML, Johansson SL, Singh RK. Distinct expression of CXCL8 and its receptors CXCR1 and CXCR2 and their association with vessel density and aggressiveness in malignant melanoma. Am J Clin Pathol 2006;125:209–16. [PubMed: 16393674]
41. Varney ML, Li A, Dave BJ, Bucana CD, Johansson SL, Singh RK. Expression of CXCR1 and CXCR2 receptors in malignant melanoma with different metastatic potential and their role in interleukin-8 (CXCL-8)-mediated modulation of metastatic phenotype. Clin Exp Metastasis 2003;20:723–31. [PubMed: 14713106]
42. Li A, Varney ML, Singh RK. Expression of interleukin 8 and its receptors in human colon carcinoma cells with different metastatic potentials. Clin Cancer Res 2001;7:3298–304. [PubMed: 11595728]
43. Reiland J, Furcht LT, McCarthy JB. CXC-chemokines stimulate invasion and chemotaxis in prostate carcinoma cells through the CXCR2 receptor. Prostate 1999;41:78–88. [PubMed: 10477904]
44. Metzner B, Hofmann C, Heinemann C, et al. Over-expression of CXC-chemokines and CXC-chemokine receptor type II constitute an autocrine growth mechanism in the epidermoid carcinoma cells KB and A431. Oncol Rep 1999;6:1405–10. [PubMed: 10523720]
45. Folberg R, Hendrix MJ, Maniotis AJ. Vasculogenic mimicry and tumor angiogenesis. Am J Pathol 2000;156:361–81. [PubMed: 10666364]
46. Shen H, Schuster R, Stringer KF, Waltz SE, Lentsch AB. The Duffy antigen/receptor for chemokines (DARC) regulates prostate tumor growth. FASEB J 2006;20:59–64. [PubMed: 16394268]

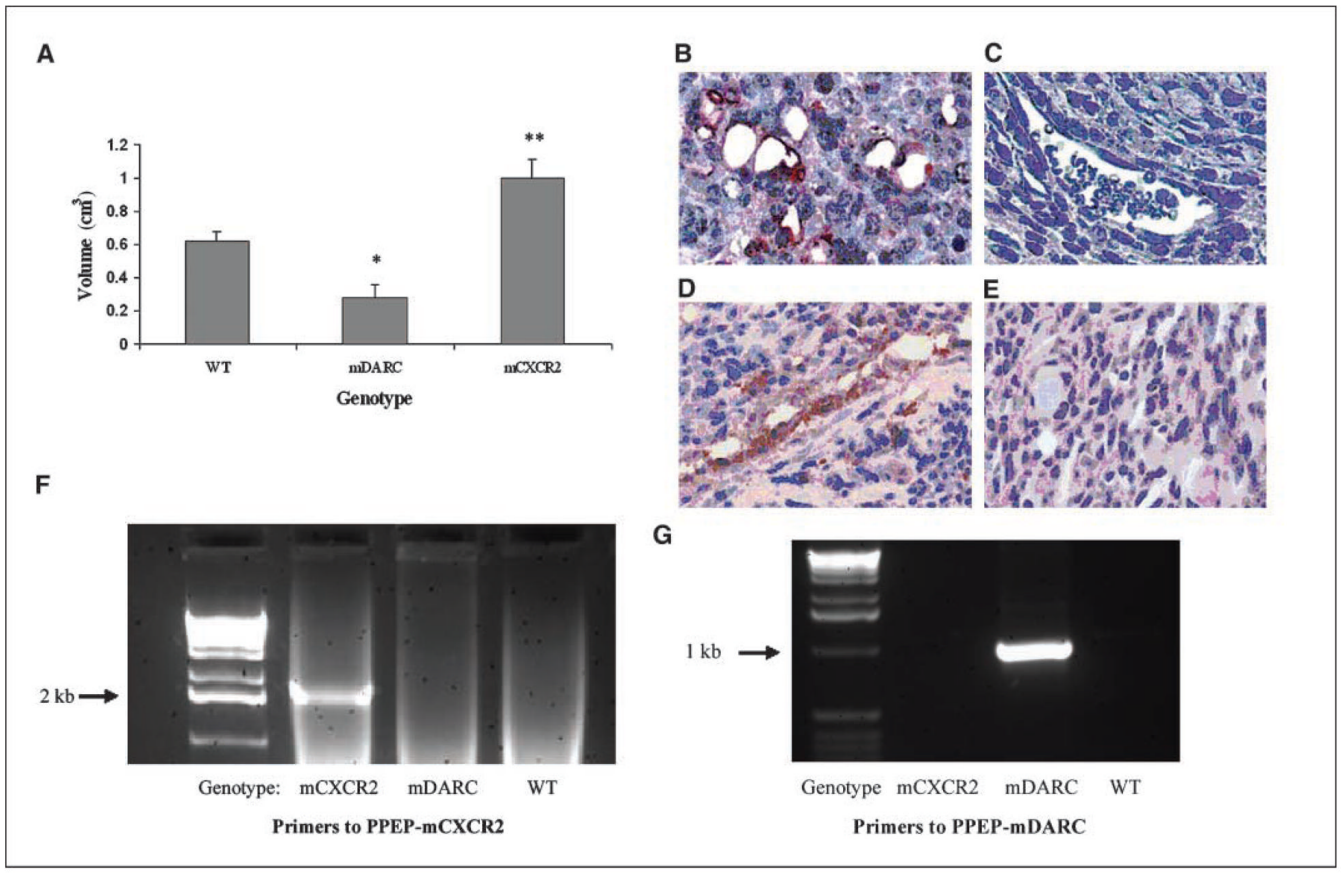

Figure 1.

A, Mela-MIP-2^{+} cells (10×10^6/200 μL/PBS) were injected s.c. into WT, PPEP-mCXCR2, and PPEP-mDARC mice. Tumors were excised from all mice at the time point at which the first tumor reached maximum size in any dimension (1.5 cm). In two independent experiments, these time points were 41 and 45 d, respectively. Tumor volume was determined by fluid displacement. The graph shows the mean tumor volume of all tumors from all mice included in both experiments. The Student's *t* test was used to evaluate the statistical significance of variance between the groups of mice. *, $P < 0.05$; **, $P < 0.005$. Confirmation of overexpression of the transgenes mCXCR2 and mDARC in melanoma tumors growing on transgenic using polyclonal antibodies directed against mCXCR2 or mDARC. Immunolocalization of mCXCR2 in melanoma tumor xenografts derived from the PPEP-mCXCR2 mouse *B* compared with CXCR2 expression in WT mice *C* based on staining with polyclonal antibody to mCXCR2. Immunolocalization of mDARC in melanoma tumor xenografts derived from the PPEP-DARC mice *D* compared with mDARC staining in tumor xenografts from WT mice *E*, stained with polyclonal antibody to mDARC. Magnification, ×40. PCR confirmation of transgene expression in the PPEP-mCXCR2 and PPEP-mDARC founder lines: PCRs were done on mouse tail DNA using protocols described in Materials and Methods. Primer sets were designed to detect transgene only and not endogenous mCXCR2 or mDARC. *F*, electrophoretic profile of products from the PCR using primers to the PPEP-mCXCR2 transgene show expression only in the CXCR2 transgenic mice. *G*, electrophoretic profile of products from the PCR using primers to PPEP-mDARC show expression only in the mDARC transgenic mice.

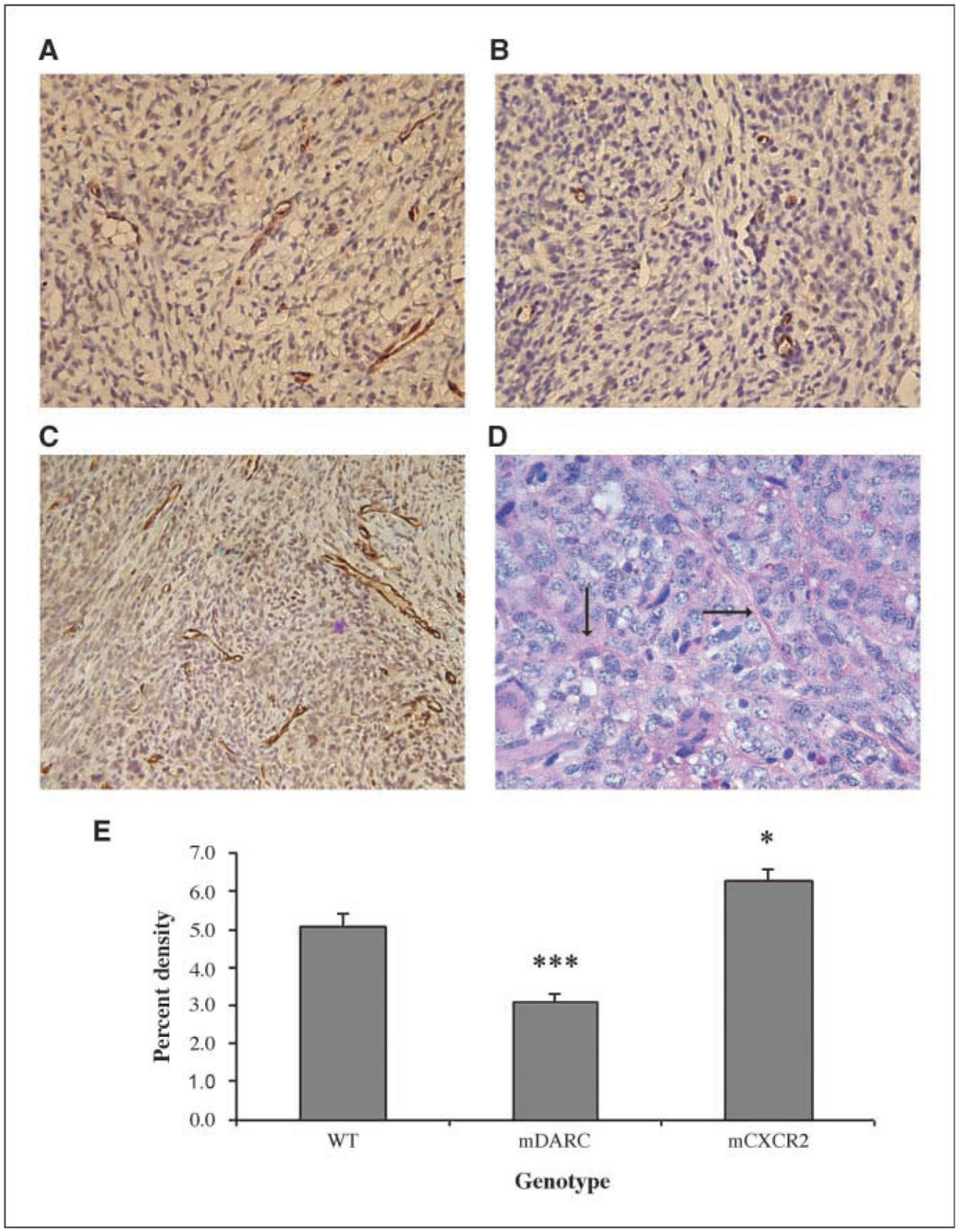

Figure 2.

Evaluation of the vascular supply in the tumors arising on PPEP-mCXCR2, PPEP-mDARC, and WT mice. Fixed tumor tissues were immunostained using antibody to PECAM-1 (CD31) to detect blood vessels. *A*, CD31 staining of vessels in Mela-MIP-2$^+$ melanoma tumors arising on WT mice. *B*, Mela-MIP-2$^+$ tumors from PPEP-mDARC mice show a marked decrease in blood vessel formation over that seen in the WT control. *C*, Mela-MIP-2$^+$ tumors from PPEP-mCXCR2 transgenic mice show a significant increase in vessel formation over that seen in the WT control. Images are representative of a minimum of 10 fields per tumor for each tumor from each experiment. *D*, tumors from PPEP-CXCR2 transgenic mice stained with PAS indicate a network of small microvessels (*arrows*). *E*, graph representation of vessel density

of all tumors included in both experiments using the quantification method described in Materials and Methods. The Student's *t* test was used to evaluate the statistical significance of variance between the groups of mice. ***, $P < 0.0005$; *, $P < 0.05$. Magnification, ×40.

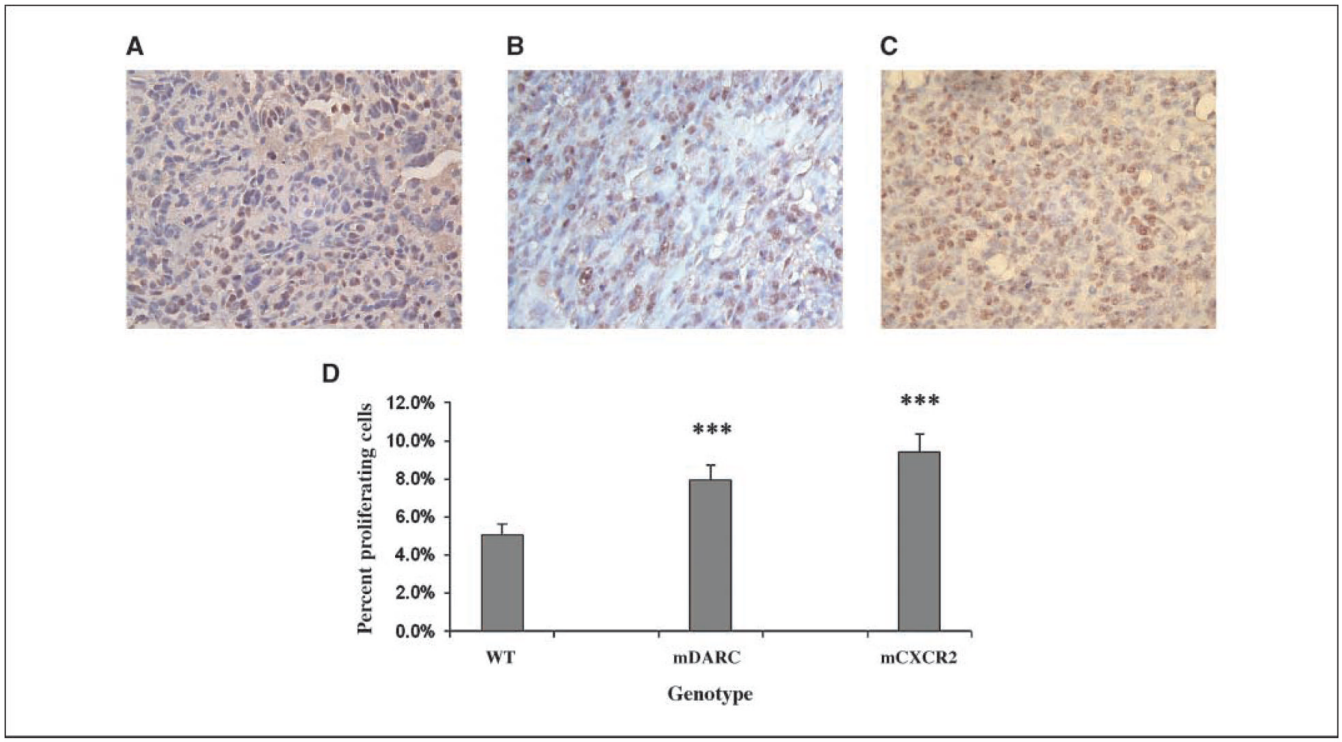

Figure 3.

Evaluation of the proliferative index of tumor cells growing on transgenic and WT mice. Paraformaldehyde-fixed, paraffin-embedded tissue sections were immunostained for PCNA. *A*, PCNA immunostaining of tumor sections from WT mice. *B*, PCNA immunostaining of tumor sections from PPEP-mDARC transgenic mice is significantly higher from that of the tumor sections from WT mice. *C*, PCNA immunostaining of tumor sections from PPEP-mCXCR2 transgenic mice showed a highly significant increase in the number of proliferating cells over that seen in the WT mice. *D*, graph representation of proliferating cells of all tumors included in both experiments using the quantification method described in Materials and Methods. The Student's *t* test was used to evaluate the statistical significance of variance between the groups of mice. ***, $P < 0.0005$. Magnification, ×40.

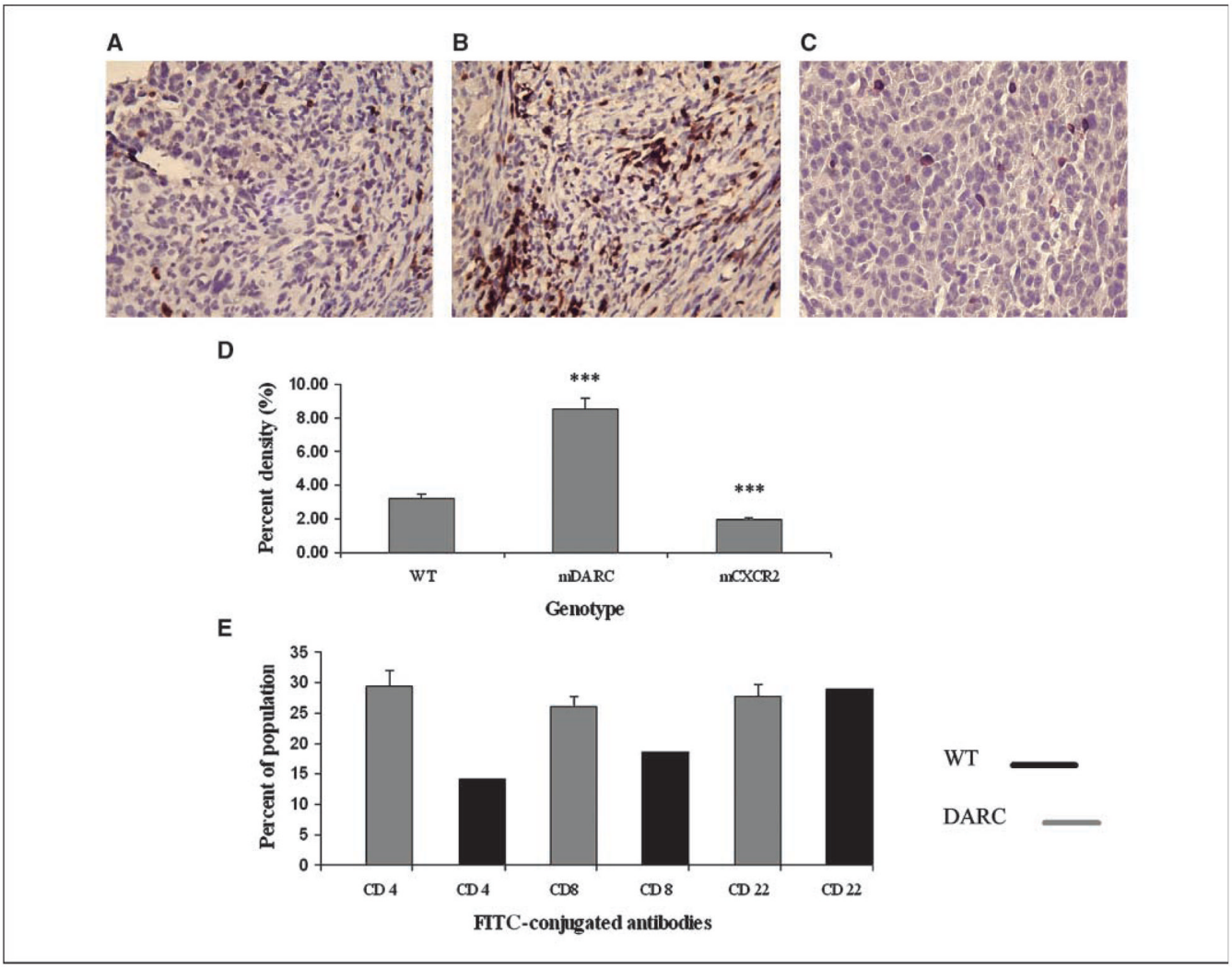

Figure 4.

Evaluation of lymphocytic infiltration into the melanoma tumors. Tumor sections were stained with a pan-lymphocyte stain (CD3/45) for total lymphocytes. *A*, mela-MIP-2^+ tumors from WT mice were used as the control group. *B*, Mela-MIP-2^+ tumors from PPEP-mDARC transgenic mice show a significant increase in lymphocyte cell density over that observed in the WT mice. *C*, Mela-MIP-2^+ tumors from PPEP-mCXCR2–overexpressing mice show a marked decrease in lymphocyte cell density over that seen in the WT mice. Images are representative of a minimum of 10 fields per tumor for each tumor from each experiment. *D*, graphic representation of the mean lymphocyte density of all tumors from all genotypes in both experiments. The Student's *t* test was used to evaluate the statistical significance of the mean lymphocyte density. ***, $P < 0.005$. Magnification, ×40. *E*, quantitation of FACS analysis of leukocytes in tumors from mDARC transgenic mice and WT littermates. The mean of the three mDARC tumor populations was compared with the WT tumor population. Results indicate that although the B-cell population is essentially the same between both tumor types, there is a marked increase in the number of T cells, both cytotoxic T cells and T_h cells in the mDARC-overexpressing tumor compared with that observed in the WT tumor.

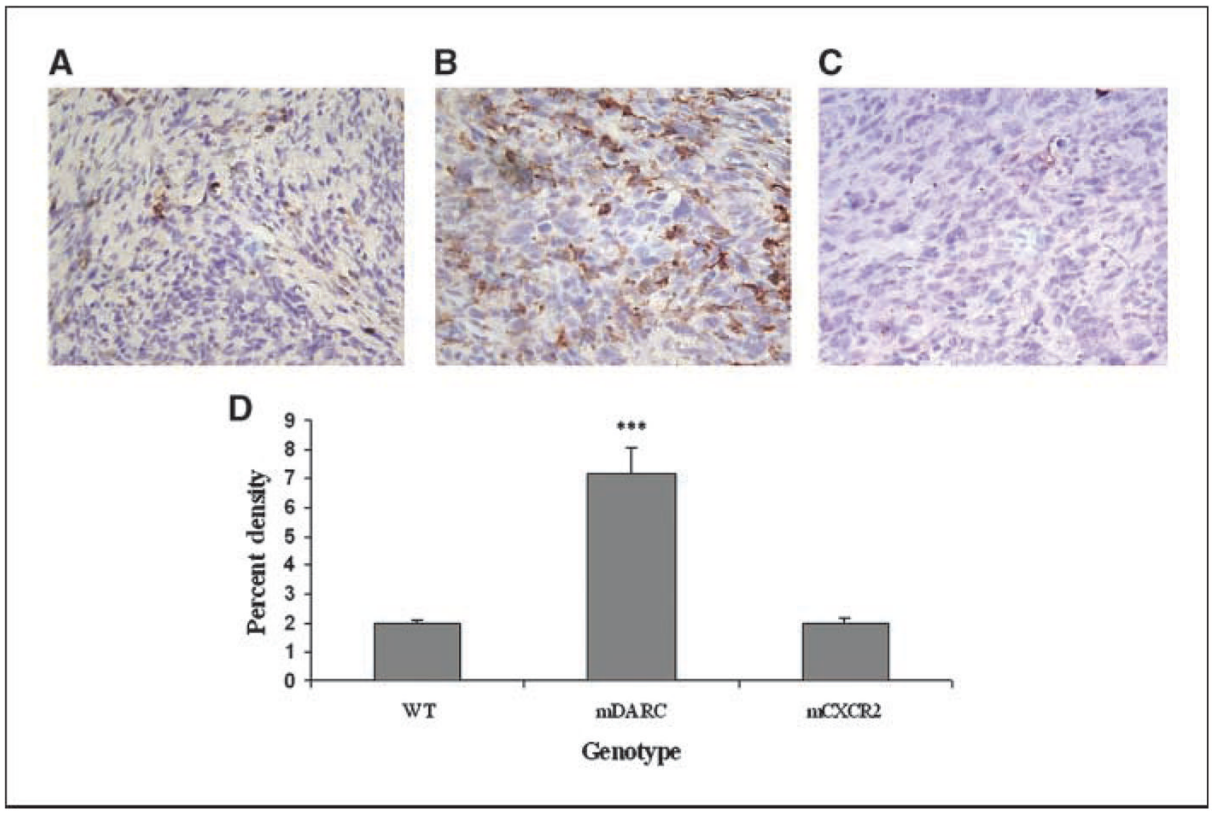

Figure 5.

Sections of tumor were stained with F4/80 to determine the density of macrophages in tumors arising in the three genotypes. *A*, the WT group served as a control for the experiment. *B*, the Mela-MIP-2^{+} tumors from the PPEP-mDARC transgenic mice showed a highly significant increase in macrophage density over that seen in the WT mice. *C*, there was no significant difference in the number of macrophages in the PPEP-mCXCR2 transgenic mice bearing Mela-MIP-2^{+} tumors. Images are representative of 10 fields per tumor counted. *D*, a graph showing a summary of the macrophage density in all tumors in each genotype for both experiments. The Student's *t* test was used to determine significance. ***, $P < 0.005$. Magnification, ×40.